



Research article

Analysis of Caputo fractional-order model for COVID-19 with non-pharmaceutical interventions and vaccine hesitancy

Mlyashimbi Helikumi¹, Paride O. Lolika^{2,*} and Steady Mushayabasa³

¹ Mbeya University of Science and Technology, Department of Mathematics and Statistics, College of Science and Technical Education, P.O. Box 131, Mbeya, Tanzania

² University of Juba, Department of Mathematics, P.O. Box 82 Juba, Central Equatoria, South Sudan

³ Department of Mathematics & Computational Sciences, University of Zimbabwe, P.O. Box MP 167, Harare, Zimbabwe

* **Correspondence:** Email: parideorest@yahoo.com; Tel: +211924606100.

Abstract: In this paper, we propose a fractional order Coronavirus (COVID-19) model incorporating non-pharmaceutical interventions and vaccine hesitancy. The proposed model was calibrated with data from literature and validated with reported daily cases of COVID-19 from Wuhan, China. We derived the reproduction number and demonstrated that it is an important threshold parameter for disease persistence and extinction. We examined the relationship between the reproduction number and model parameters. Our findings underscore the importance of awareness and vaccine uptake on mitigating the spread of COVID-19.

Keywords: COVID-19; mathematical model; Caputo derivative; non-pharmaceutical interventions; vaccine hesitancy; simulations

1. Introduction

Emerging and re-emerging infectious diseases remains a major public health concern. In the last four years, the world witnessed an unprecedented outbreak of coronavirus disease (COVID-19). Since its discovery, COVID-19 has been swiftly spreading from one country to another causing massive deaths and economic devastation world wide. As of 4 June 2023, the cumulative reported number of confirmed cases of COVID-19 reached over 767 million and the cumulative number of deaths reaches over 6.9 million deaths globally [1]. Despite significant progress in the development and introduction of new diagnostics, which has lead to a remarkable decline in deaths and new infections, COVID-19 remains a public health challenge. According to the latest estimates from the world health organization (WHO), from 8 May to 4 June 2023 (28 days), over 1.7 million new cases and over 10,000 deaths

occurred globally [1]. Compared to the previous 28 days (10 April to 7 May 2023), this represents a decrease of 38% and 47% in cases and deaths, respectively [1].

In spite of a considerable decline in COVID-19 cases and deaths, it remains imperative for researchers to continuously explore the strength of the novel control methods to eradicate the disease. Mathematical models provide powerful tools for explaining and predicting the COVID-19 trend, and also for quantifying the effectiveness of different novel control strategies either singly or combined. Since its discovery, several mathematical models have been formulated to extensively study various aspects of factors involving COVID-19 transmission and control. Ndairou et al. [2] employed a system of integer ordinary differential equations (IODEs) to model the effects of super-spreaders on COVID-19 dynamics in Wuhan, China. Findings from their work showed that super-spreaders play a crucial role on the generation of secondary infections.

Rozenfeld et al. [3] proposed a statistical model to evaluate risk factors associated with COVID-19 infection. Their study showed that the risk of COVID-19 infection is higher among groups already affected by health disparities across age, race, ethnicity, language, income and living conditions. Mushayabasa et al. [4] developed a mathematical model based on IODEs to evaluate the role of governmental action and individual reaction on COVID-19 dynamics in South Africa. Their study demonstrated optimal conditions necessary for the infection to die out as well as persist. In [5], a system of IODEs were utilized to investigate the impacts of vaccination on COVID-19 dynamics. They concluded that vaccination could significantly reduce the generation of new infections. To explore the impact of lockdown of COVID-19 transmission dynamics, Ahmed et al. [6] developed a mathematical model based on the Caputo fractional-order. Khan et al. [7] presented a compartmental model based on Caputo-Fabrizio operator to predict COVID-19 dynamics in the Sultanate of Oman. Ghosh and Martcheva [8] developed an epidemic model based on IODEs to investigate the effects of prosocial awareness on COVID-19 dynamics in Colombia and India. Results from their work showed that prosocial awareness has competitive potential to flatten the COVID-19 prevalence curve.

The aforementioned mathematical models of COVID-19 and those cited therein have certainly produced many useful results and improved the existing knowledge on the disease dynamics. However, despite all these efforts, several challenges remain in the mathematical modeling of COVID-19. In particular, since the advent of several COVID-19 vaccines, a large proportion of the population in different parts of the globe has been reluctant to be inoculated [9–11]. This phenomena is known as vaccine hesitancy. WHO defines vaccine hesitancy as the delay in acceptance or refusal of vaccines despite the availability of vaccine services [12]. Vaccine hesitancy limits vaccine efficacy [9].

Emperical studies have shown that the average acceptance rates of the COVID-19 vaccines are relatively low across the world, particularly in the Middle East, Russia, Africa and several European countries [9]. In particular, a study conducted in France in October 2020 revealed that 46% of French citizens are vaccine hesitant. Furthermore, studies conducted in other countries revealed the following statistics with regards to COVID-19 vaccine hesitancy: 36% in Spain and USA, 35% in Italy, 32% in South Africa and 31% in Japan and Germany. Globally, vaccine hesitancy and objection has been estimated to be around 27% [13]. Lack of information about the side effects, especially the long-term effects, time-line of the COVID vaccines production, culture and religion issues, political and conspiracy theory, are some of the reasons that have been associated with vaccine hesitancy [9, 10].

Considering these large percentages of hesitance and objection of COVID-19 vaccines, we thought it is prudent to quantify the public health implications of vaccine hesitancy on COVID-19 dynamics. To

this end, we developed a mathematical model of COVID-19 transmission that incorporates vaccination effects and non-pharmaceutical interventions (NPIs). Since vaccination is voluntary and most of the COVID-19 vaccines require two or more doses for one to be completely vaccinated, we assume that individuals can choose to be partially or completely vaccinated. Partially vaccinated individuals are those that do not complete all the required vaccine doses while completely vaccinated are those that complete all the required doses per vaccine.

In this study, we are particularly concerned with quantifying the effects of delaying the first and second COVID-19 vaccine dose on disease dynamics. We are cognisant that the Joint Committee on Vaccination and Immunisation (JCVI) recommends the second dose from 3 to 12 weeks after the first dose [14]. Hence, we will evaluate the implications of taking the second dose after 12 weeks (approximately 84 days). Quantifying the effects of interventions enable policy maker and health experts to evaluate the success of an epidemic response so as to improve and inform ongoing and future interventions.

We therefore proposed a mathematical framework based on the Caputo Fractional derivative, since fractional models can more accurately describe biological and natural phenomena than integer ordinary differential equations [15–17]. Although there are several fractional derivatives in literature, we have employed the Caputo derivative due to the following reasons (i) the Caputo derivative for a constant has the same outcome as that of an integer ordinary differential equation, (ii) computations based on the Caputo derivative makes use of local initial conditions, and (iii) the Caputo operator computes an ordinary differential equation, followed by a fractional integral to obtain the desired order of fractional derivative [18–20]. To the best of our knowledge, there are no studies in literature that have attempted to quantifying the effects of delaying the second COVID-19 vaccine dose using a fractional model.

The rest of the paper is organized as follows: Section 2 presents the material and methods. We present the novel COVID-19 model and its assumptions. Section 3 presents the results and discussions. In particular, we present both analytical and numerical findings. Finally, concluding remarks and limitations rounds up the paper.

2. Materials and methods

In this section, we present a fractional model to study the transmission of COVID-19 incorporating NPIs use and vaccination. The model is based on Fractional Calculus (FC), in particular, the Caputo derivative and the Caputo fractional derivative of order q is defined by equation (2.1) [21]:

$$D_{t_0}^q x := \begin{cases} \frac{1}{\Gamma(1-q)} \int_0^t \frac{\dot{x}}{(t-\tau)^q} d\tau, & 0 < q < 1, \\ \frac{d}{dt} x(t), & q = 1 \end{cases} \quad (2.1)$$

with $t > 0$, $q \in (0, 1]$.

2.1. Mathematical model

Let $S(t)$, $V(t)$, $E(t)$, $I(t)$, $A(t)$, $H(t)$ and $R(t)$ denote the number of susceptible, vaccinated, exposed, clinically infected, asymptomatic infectious patients, hospitalized, and recovered human at time t ,

respectively. Thus the total human population at time t is given by $N(t) = S(t) + V(t) + E(t) + I(t) + A(t) + H(t) + R(t)$. The model is formulated based on the following assumptions:

- (i) All new recruited individuals are assumed to be susceptible to infection. Let Λ be the constant recruitment rate. Susceptible individuals are assumed to acquire infection following effective contact with individuals displaying clinical signs of the disease $I(t)$, asymptomatic infectious patients $A(t)$ and hospitalized patients $H(t)$. Thus, consider the following force of infection $\lambda_h(t) = \beta(1 - \epsilon)(H + A + I)$, where β is the infection rate and ϵ ($0 \leq \epsilon < 1$) accounts for the effectiveness of NPIs to reduce disease transmission.
- (ii) Susceptible individuals are assumed to receive their first dose at rate κ . Thus $1/\kappa$ accounts for the delay in taking the first COVID-19 vaccine dose. We assume that individuals inoculated with the first dose have reduced chances of contracting the disease. Thus, partially vaccinated individuals can acquire infection at rate $(1 - \phi)\lambda_h(t)$, where ϕ ($0 \leq \phi < 1$) accounts for vaccine efficacy. If $\phi \approx 1$, it implies that the vaccine is highly effective and $\phi \approx 0$, implies that the vaccine is ineffective. COVID-19 led to the advent of several vaccines. Pfizer-BioNTech, Moderna, Sinopharm, Sinovac, Sputnik V, Janssen (Johnson & Johnson's) and AstraZeneca are some of the companies that developed COVID-19 [22]. Although these vaccines were found to be effective to prevent COVID-19, their levels of efficiency varies. However, for most of these vaccines, experimental and field studies have shown that for a higher efficiency, optimal vaccine doses need to be more than one. Hence, in this study, we assume that vaccinated individuals who receive the recommended doses relative to the vaccine being administered (more than a single dose) are removed from infection at rate θ_2 . Thus, $1/\theta_2$ accounts for the delay in taking the second COVID-19 vaccine dose.
- (iii) Upon being infected with COVID-19, individuals enter the exposed state. These individuals incubate the disease and are not yet infectious. We assume that they will remain in this state for an average period of $1/\alpha$ days, after which a proportion ω develop clinical signs of the disease and the remainder $1 - \omega$ becomes asymptomatic infectious patients. Clinically infected and asymptomatic infectious patients are detected and hospitalized at rates δ_1 and δ_2 , respectively. Asymptomatic infectious and clinically infected patients receiving home based care are assumed to recover at rates γ_1 and γ_2 , respectively. Furthermore, clinically infected and hospitalized COVID-19 patients are assumed to suffer disease-related mortality at rate d . Successfully treated hospitalized patients recover from the disease at rate γ_3 . In addition, we assume that natural mortality occurs in all epidemiological classes at a constant rate μ .

Based on the above assumptions the transmission dynamics of COVID-19 can be summarized by the following system of equation (Model flow diagram is in Figure 1):

$$\left. \begin{aligned}
 D_{t_0}^q S(t) &= \Lambda^q - \beta^q(1 - \epsilon)(H + A + I)S - (\mu^q + \kappa^q)S, \\
 D_{t_0}^q V(t) &= \kappa^q S - \beta^q(1 - \phi)(1 - \epsilon)(H + A + I)V - (\mu^q + \theta_2^q)V, \\
 D_{t_0}^q E(t) &= \beta^q(1 - \epsilon)(H + A + I)(S + (1 - \phi)V) - (\alpha^q + \mu^q)E, \\
 D_{t_0}^q A(t) &= (1 - \omega)\alpha^q E - (\mu^q + \gamma_1^q + \delta_2^q)A, \\
 D_{t_0}^q I(t) &= \omega\alpha^q E - (\mu^q + d^q + \gamma_2^q + \delta_1^q)I, \\
 D_{t_0}^q H(t) &= \delta_2^q A + \delta_1^q I - (\mu^q + d^q + \gamma_3^q)H, \\
 D_{t_0}^q R(t) &= \gamma_1^q A + \gamma_2^q I + \gamma_3^q H + \theta_2^q V - \mu^q R.
 \end{aligned} \right\} \quad (2.2)$$

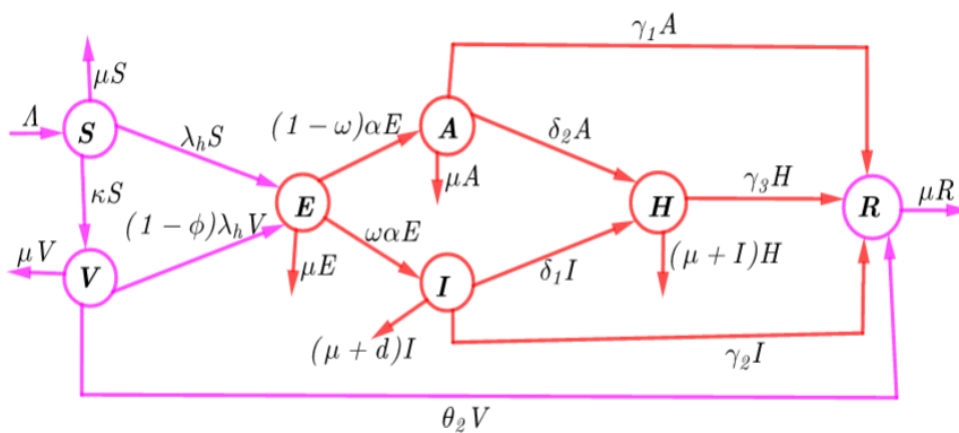


Figure 1. A transition diagram between epidemiological classes.

3. Results and discussions

In this section, we present both analytical and numerical results.

3.1. Non-negativity and boundedness of model solutions

Since model (2.2) monitors human population, it is essential to demonstrate that all model solutions are bounded and positive for all $t \geq 0$. Based on the computations in Supplement A, we obtained the following results.

Theorem 3.1. *Model (2.2) has unique and non-negative solutions which turn into region Ω_+ as $t \rightarrow \infty$, where Ω_+ is defined by:*

$$\Omega_+ = \left\{ (S, V, E, A, I, H, R) \in \mathbb{R}_+^7 \mid \begin{aligned} &S \geq 0, V \geq 0, E \geq 0, I \geq 0, A \geq 0, H \geq 0, R \geq 0, \\ &S + V + E + A + I + H + R = N \leq \Lambda^q / \mu^q, \end{aligned} \right\} \quad (3.1)$$

3.2. Reproduction numbers

One of the most important threshold quantity of epidemiological models is the reproduction number. It demonstrates the disease transmission potential during an outbreak. Generally, the reproduction number is defined as the average number of new infections produced by a typical infected individual during their entire infectious period when introduced into a completely susceptible population [23]. To determine the reproduction number we will make use of the Next-generation matrix (NGM) method [24]. Based on the computations in Supplement B, we obtained the expression of reproduction number of model (2.2) as follows (3.2):

$$\begin{aligned} \mathcal{R}_0 &= \beta^q(1-\epsilon)(1-\omega)\left(\frac{\Lambda^q}{\mu^q + \kappa^q} + \frac{\kappa^q(1-\phi)\Lambda^q}{(\kappa^q + \mu^q)(\mu^q + \theta_2^q)}\right)\frac{\alpha^q}{(\alpha^q + \mu^q)(\mu^q + \gamma_1^q + \delta_2^q)} \\ &\quad + \beta^q(1-\epsilon)\omega^q\left(\frac{\Lambda^q}{\mu^q + \kappa^q} + \frac{\kappa(1-\phi)\Lambda}{(\kappa + \mu)(\mu + \theta_2)}\right)\frac{\alpha}{(\alpha^q + \mu^q)(\mu^q + d^q + \gamma_2^q + \delta_1^q)} \\ &\quad + \frac{\beta^q(1-\epsilon)\alpha^q}{(\alpha^q + \mu^q)(\mu^q + d^q + \gamma_3^q)}\left(\frac{\Lambda^q}{\mu^q + \kappa^q} + \frac{\kappa^q(1-\phi)\Lambda^q}{(\kappa^q + \mu^q)(\mu^q + \theta_2^q)}\right)\left(\frac{(1-\omega)\delta_2^q}{(\mu^q + \gamma_1^q + \delta_2^q)} + \frac{\omega\delta_1^q}{(\mu^q + d^q + \gamma_2^q + \delta_1^q)}\right) \\ &= \mathcal{R}_{0A} + \mathcal{R}_{0I} + \mathcal{R}_{0H}, \end{aligned} \quad (3.2)$$

where \mathcal{R}_{0j} , for $j = A, I, H$ denotes the average number of secondary infections generated by one infectious individual from epidemiological class j introduced in population wholly of susceptible (vaccinated and unvaccinated) humans. From (3.2) one can observe the totally susceptible (vaccinated and unvaccinated) human population, $\frac{\Lambda^q}{\mu^q + \kappa^q} + \frac{\kappa^q\Lambda^q}{(\kappa^q + \mu^q)(\mu^q + \theta_2^q)}$, contracts the disease following contact with infected individuals in classes A, I and H at rate β^q . Disease transmission is assumed to be reduced by human awareness, $(1-\epsilon)$. Susceptible vaccinated individuals have lesser chances of contracting the disease compared to susceptible unvaccinated, modelled by a factor $1-\phi$. Infected individuals have the probability $\frac{\alpha^q}{(\alpha^q + \mu^q)}$ to survive the exposed state to become infectious. A proportion $(1-\omega)$ of infected individuals that survive the exposed state will become infectious for an average duration of $\frac{1}{(\mu^q + \gamma_1^q + \delta_2^q)}$. The complementary proportion ω , which survive the exposed state and become clinical patients will be infectious for an average period $\frac{1}{(\alpha^q + \mu^q)(\mu^q + d^q + \gamma_2^q + \delta_1^q)}$. Asymptomatic infectious patients detected at rate δ_2^q are hospitalized and will be infectious for an average period $\frac{1}{(\mu^q + \gamma_1^q + \delta_2^q)}$. Clinically infected patients detected at rate δ_1^q are hospitalized and their average infectious duration is $\frac{1}{(\mu^q + d^q + \gamma_2^q + \delta_1^q)}$.

3.3. Stability of the model steady states

The main focus of this section is to analyze the global behavior of model (2.2) by examining its stability. Global stability analysis enables the researcher to understand the evolution of the disease about the model steady states. Comprehensive analysis in Supplement C shows that the following result holds.

Theorem 3.2. *If $\mathcal{R}_0 < 1$ then the disease-free equilibrium (DFE) is globally stable. However, if $\mathcal{R}_0 > 1$ the DFE is unstable and a unique equilibrium exists and is a global attractor.*

Theorem 3.2 implies that whenever $\mathcal{R}_0 < 1$ the disease dies out in the community and it persists if $\mathcal{R}_0 > 1$. Hence if novel intervention strategies are capable of reducing \mathcal{R}_0 to values less than unity then the disease will become extinct.

3.4. Estimation of model parameters

In order to determine numerical results of model (2.2), we need to estimate the model parameters. We obtain these parameter values using two approaches: some parameter values are adapted from literature and some other parameter values are estimated by computing the root-mean square error (RMSE) as follows:

$$\text{RMSE} = \sqrt{\frac{1}{n} \sum_{k=1}^n (\text{Estimate} - \text{Observed cases})^2}, \quad (3.3)$$

where n is the number of observations. We will make use of the COVID-19 data for Wuhan, China presented in [2]. Note that the daily cases correspond to the first term of the equation $D_{t_0}^q H(t)$. We will use this term to estimate new daily infections of model (2.2). All model parameter values are presented in Table 1. We assumed the initial population levels as follows: $S(0) = 4000$, $V(0) = 0$, $E(0) = 10$, $I(0) = 0$, $A(0) = 0$, $H(0) = 6$, and $R(0) = 0$. From model (2.2) the daily new cases correspond to the term $\delta_2^q A + \delta_1^q I$ which account for the detected cases.

Table 1. Parameters and values.

Symbol	Description	Value	Units	Source
ω	Proportion of exposed individuals who develop clinical signs of the disease	Dimensionless	0.75	[4]
Λ	Per capita human recruitment rate	Day ⁻¹	20	[25]
α^{-1}	Incubation period	Day	2 (2–14)	[25]
ϕ	Vaccine efficacy	Dimensionless	0.5 (0–1)	[25]
κ	Rate of vaccination with first dose	Day ⁻¹	0.03	[25]
θ_2	Rate of vaccination with more than a single dose	Days ⁻¹	0.05	[25]
ϵ	Efficacy of NPIs	Dimensionless	0.5 (0-1)	[25]
δ_1	Rate of hospitalization of clinical patients	Day ⁻¹	0.94	[25]
δ_2	Rate of hospitalization of asymptomatic patients	Day ⁻¹	0.94	[25]
γ_1	Recover rate of asymptomatic humans	Day ⁻¹	0.004	[25]
γ_2	Recover rate of infected humans	Day ⁻¹	0.015	[25]
γ_3	Recover rate of hospitalized humans	Day ⁻¹	0.5	[25]
d	Disease induced death rate	Day ⁻¹	0.005	[26]
μ	Natural death rate	Day ⁻¹	5×10^{-6}	[26]
β	Disease transmission rate	Day ⁻¹	5.4×10^{-6}	Fitting

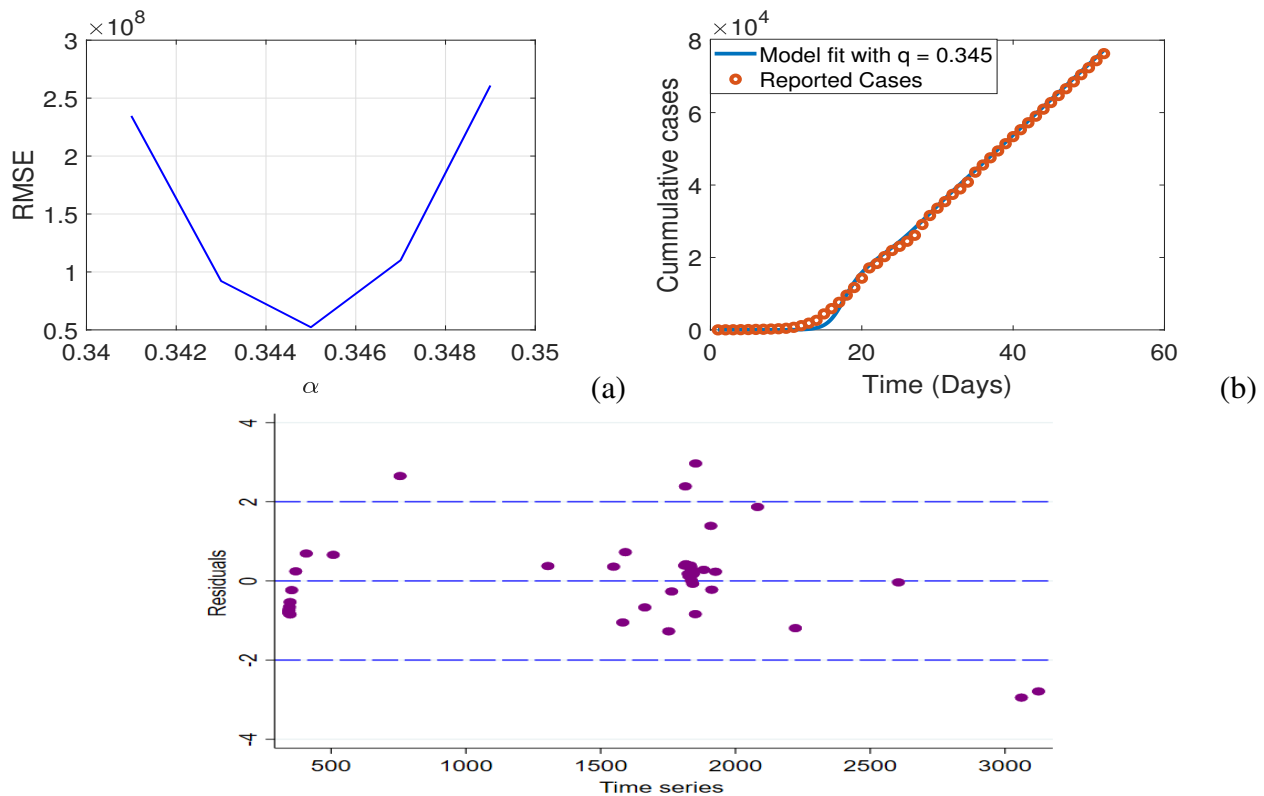


Figure 2. (a) The root-mean-square error (RMSE) for different derivative orders. The minimum error of estimation is obtained for $q = 0.345$. (b) The estimation of the fractional-order model with $q = 0.345$. (c) Plot of residuals.

Simulation results in Figure 2 shows (a) the RMSE for different derivative orders (b) model fit versus observed values and (c) plot of residuals. From the illustration in (a), one can observe that the minimum error of estimation for the given data occurs for $q = 0.345$. In (b), we can observe that model estimates are extremely close to the observed data. In (c), one can observe that the residuals show very little or no autocorrelation or partial autocorrelation an evidence that we have a good fit.

3.5. Global sensitivity analysis

We examined the relationship between individual parameters and \mathcal{R}_0 when all model parameters are simultaneously varied. We performed this analysis utilizing the partial rank correlation coefficients (PRCC) approach presented in [27], and the results are presented in Figure 3. The output shows that an increasing recruitment and disease transmission rate will increase disease transmission potential. In contrast, the simulations shows that increasing (i) NPIs use; (ii), vaccination of susceptible individuals (with either first dose or more than one dose) and vaccine efficacy will significantly reduce disease transmission potential. Together, these results suggest that reducing disease transmission rate through awareness campaigns and vaccination will significantly reduce disease transmission potential. In addition, results show that NIPs use has most impact on reducing disease transmission potential. We further investigated the relationship between \mathcal{R}_0 and four model parameters which are strongly correlated to it; awareness and disease transmission rate (Figure 4). Overall, these simulations confirm that increasing

disease transmission rate will increase disease transmission potential and increasing use of NPIs will reduce disease transmission potential.

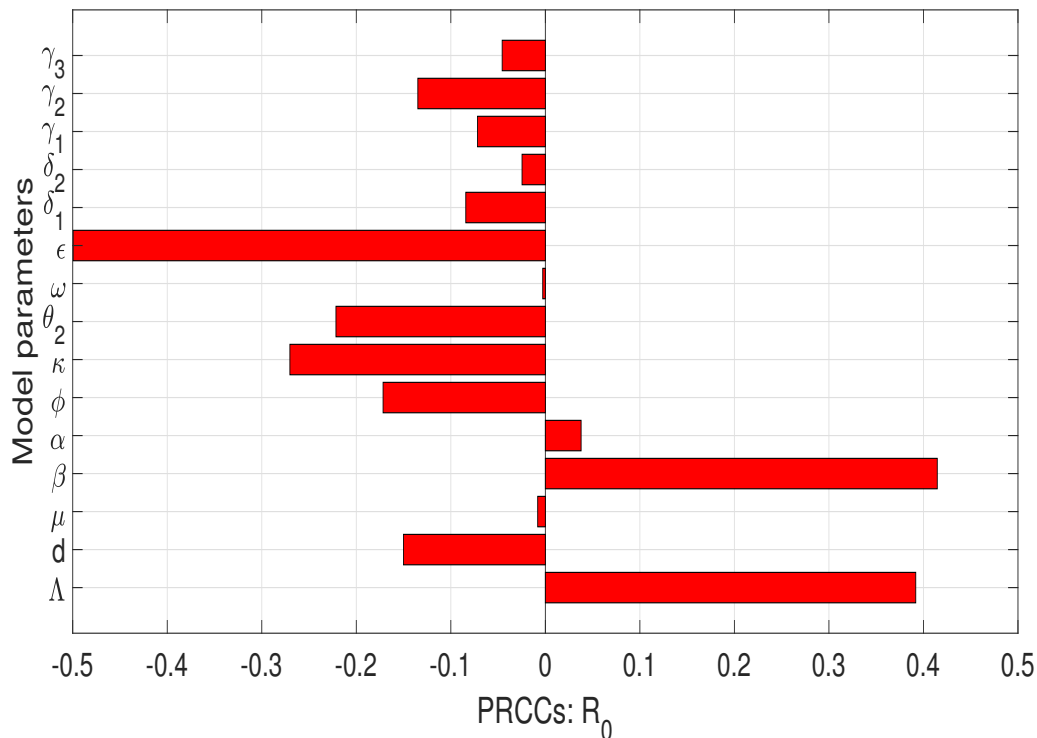


Figure 3. Sensitivity analysis of \mathcal{R}_0 with respect to its model parameters.

A contour plot of \mathcal{R}_0 as a function of ϵ (NPIs use) and ϕ (vaccine efficacy) is presented in Figure 5. The values of other model parameters are based on Table 1. We observe that whenever the efficacy of NPIs and vaccine are at least 80% all the time, then the disease transmission potential is reduced to values below unity. This implies that the disease will die out in the community as guaranteed by Theorem 3.2.

3.6. Effects of NPIs and vaccination on disease dynamics

Sensitivity analysis results have shown that high NPIs and vaccine efficacy have the potential to reduce transmission potential. Here, we examine the disease dynamics with varying vaccine and NPIs efficacy (Figure 6). Simulation results (Figure 6) concur with earlier findings that increasing NPIs use coupled with high effective vaccine will lead to disease extinction. In particular, one can observe that when both NPIs use and vaccine efficacy exceeds 75% then the disease dies out in the community. Precisely, when $\epsilon = \phi = 0$, then $\mathcal{R}_0 = 3.96$ and when $\epsilon = \phi = 75\%$, then $\mathcal{R}_0 = 0.2491$. Results presented in Figure 6 also concur with analytical results in Theorem 3.2 that if $\mathcal{R}_0 < 1$ the disease dies out and the reverse occurs for $\mathcal{R}_0 > 1$.

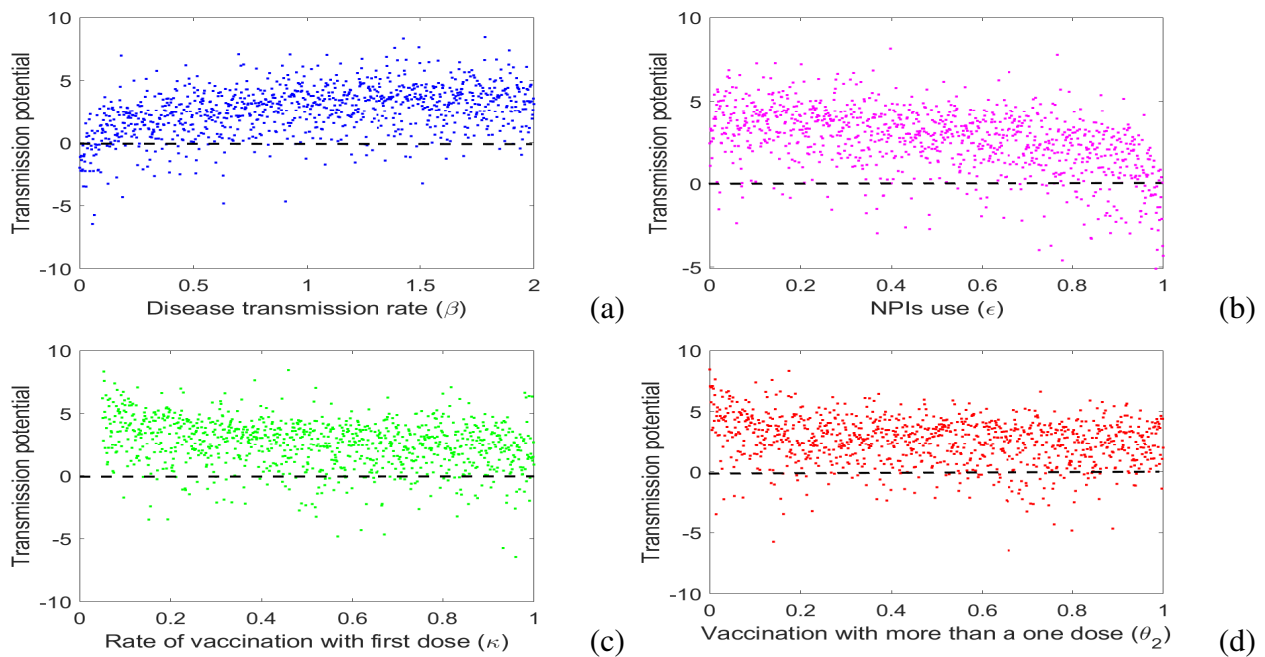


Figure 4. Monte Carlo simulations of 1000 sample values for four illustrative parameters (disease transmission rate, NPIs and vaccination rates) chosen via Latin Hypercube Sampling.

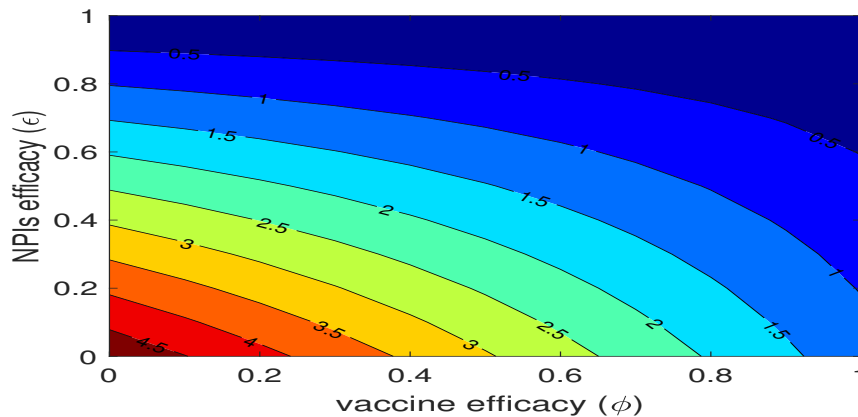


Figure 5. Contour plot of R_0 as a function of ϵ (NPIs use) and ϕ (vaccine efficacy).

3.7. Effects of delaying the first COVID-19 vaccine dose on disease dynamics

To assess the effects of delaying the uptake of the first COVID-19 vaccine dose on disease dynamics, we simulated model (2.2) at different values of κ with θ_2 fixed at 0.01 per day. The results are in Figure 7. Results show that a delay exceeding 10 days ($\kappa = 0.1$) may lead to disease persistence and the reverse leads to disease extinction.

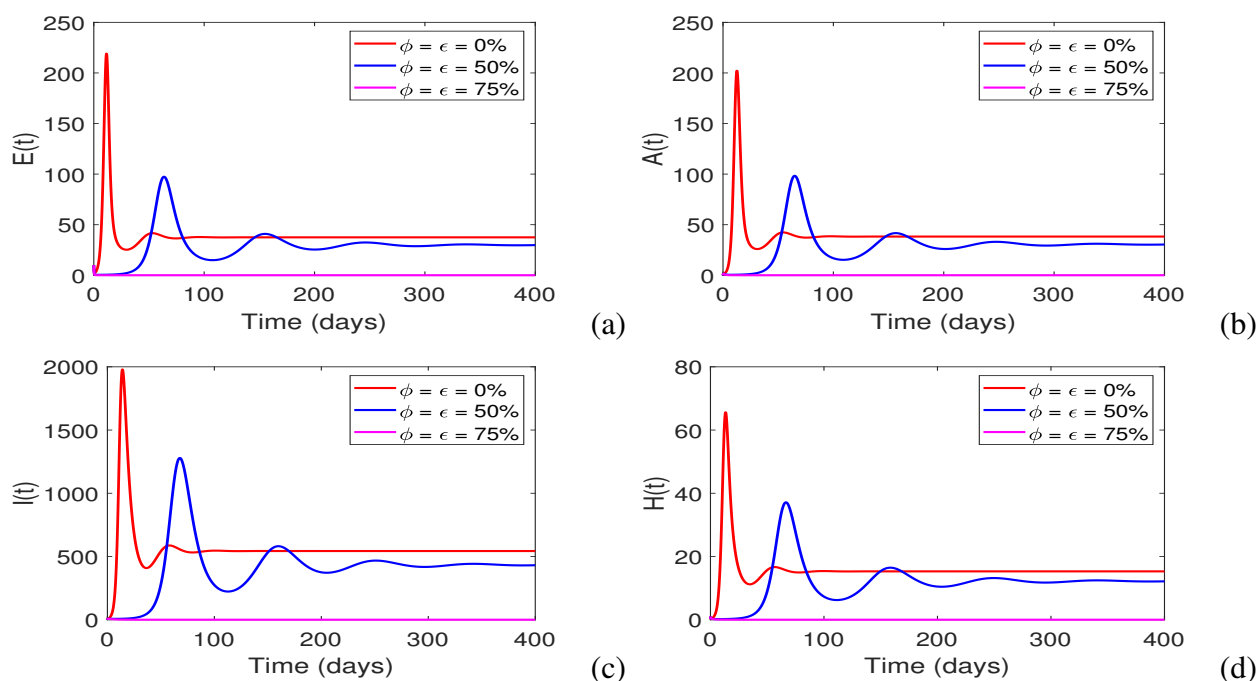


Figure 6. Effects of NPIs and vaccine efficacy on disease dynamics.

3.8. Effects of delaying the second COVID-19 vaccine dose on disease dynamics

To evaluate the effects of delaying the second COVID-19 vaccine dose on disease dynamics, we simulated model (2.2) at different values of θ_2 , (the rate at which individuals received more than a single dose) and the other model parameters are fixed as in Table 1. The results are in Figure 8. Simulation results indicates that an increase in the number of individual who take the optimal vaccine doses will lead to disease extinction. Based on these results one can conclude that, if the delay for the second COVID-19 vaccine is more than 100 days ($\theta_2 = 0.01$) then the disease may persist. Results in Figure 7 and 8 both show that delaying accepting COVID-19 vaccines have public health implications.

3.9. The role of memory effects on disease dynamics

To investigate the role of memory effects on the evolution COVID-19 over time, we simulated model (2.2) for $\mathcal{R}_0 < 1$ (Figure 9) and $\mathcal{R}_0 > 1$ (Figure 10) at different values of q (the derivative order). In all scenarios, we observed that model solutions will converge to a unique equilibrium point. In particular, if $\mathcal{R}_0 < 1$ model solutions converges to DFE and if $\mathcal{R}_0 > 1$ solution converge to a unique endemic equilibrium. Moreover, we observed that for $\mathcal{R}_0 > 1$ model solutions for different derivative orders exhibit an oscillatory behavior before they eventually converge to their respective endemic points. This phenomena was also observed in the following studies [28, 29]. In addition, we observed that due to the fractional-order the rate of decay and growth of solutions differs. In particular, when the memory effects are strong ($q < 1$), the model solutions converges to their respective equilibrium points earlier than when memory effects are weak ($q \approx 1$). This outcome was also noted in the work of Nisar et al. [30].

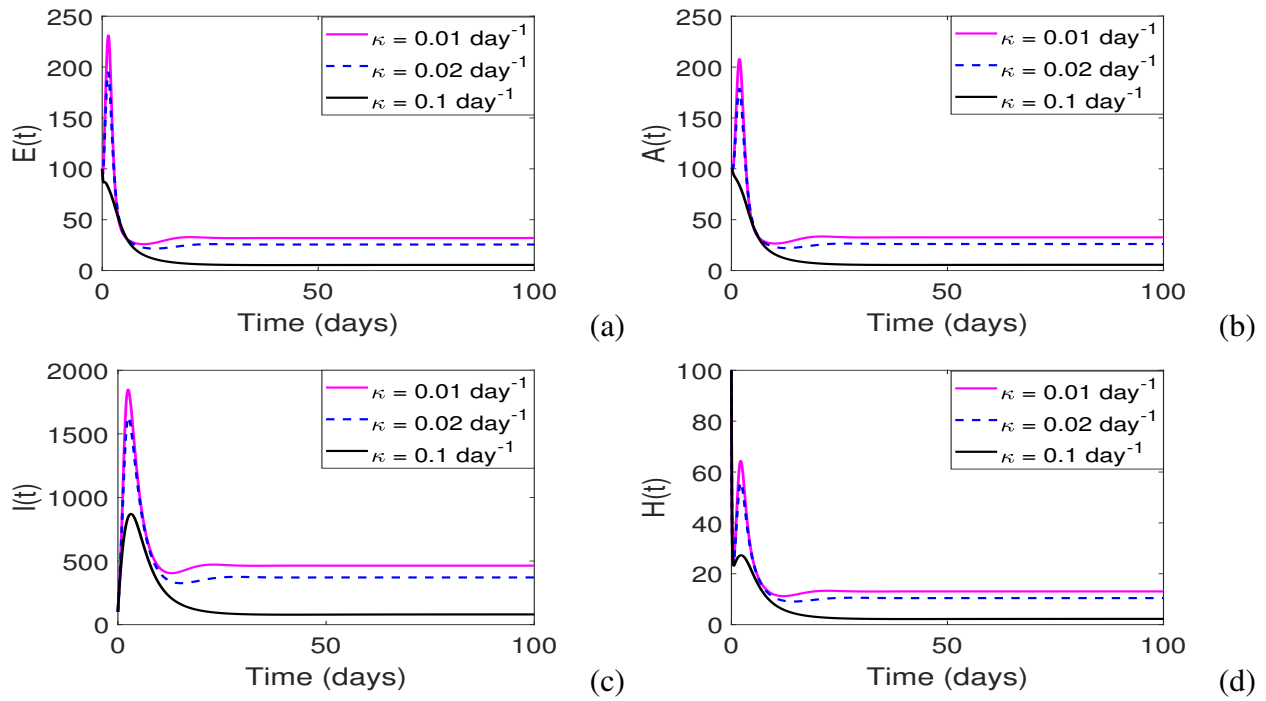


Figure 7. Effects of delaying the first COVID-19 vaccine dose on disease dynamics.

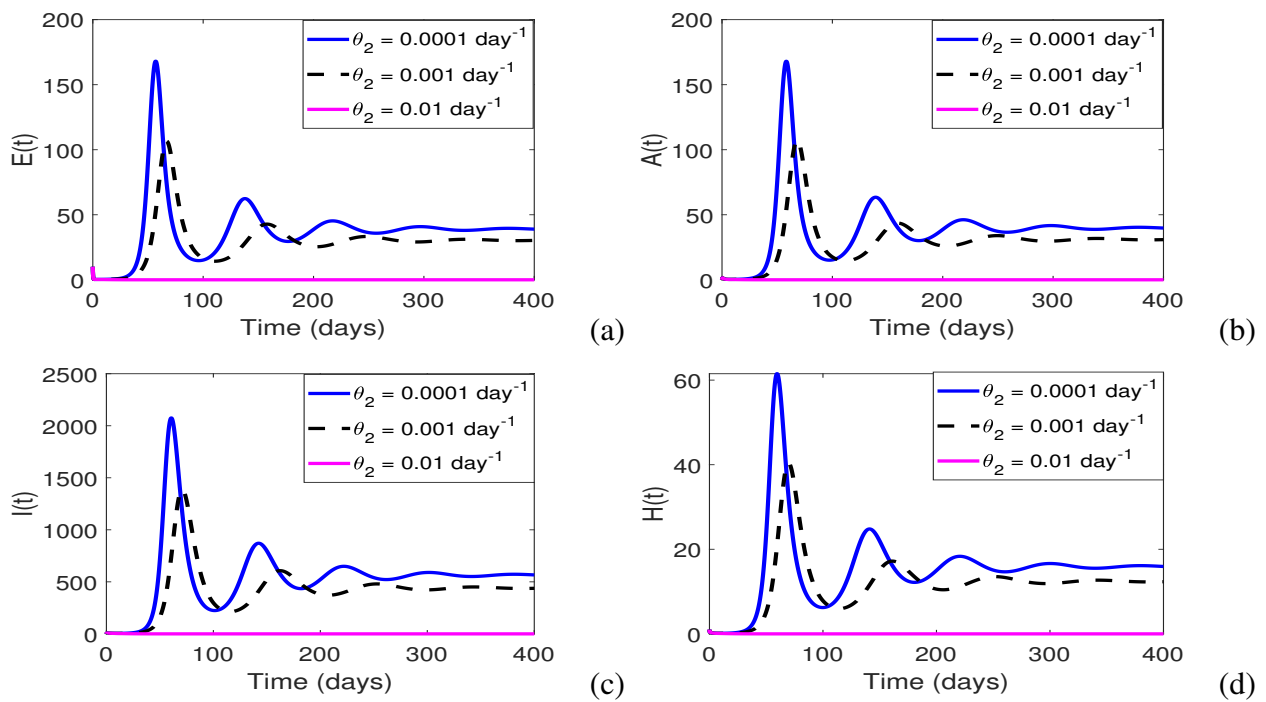


Figure 8. Effects of delaying the second COVID-19 vaccine dose on disease dynamics.

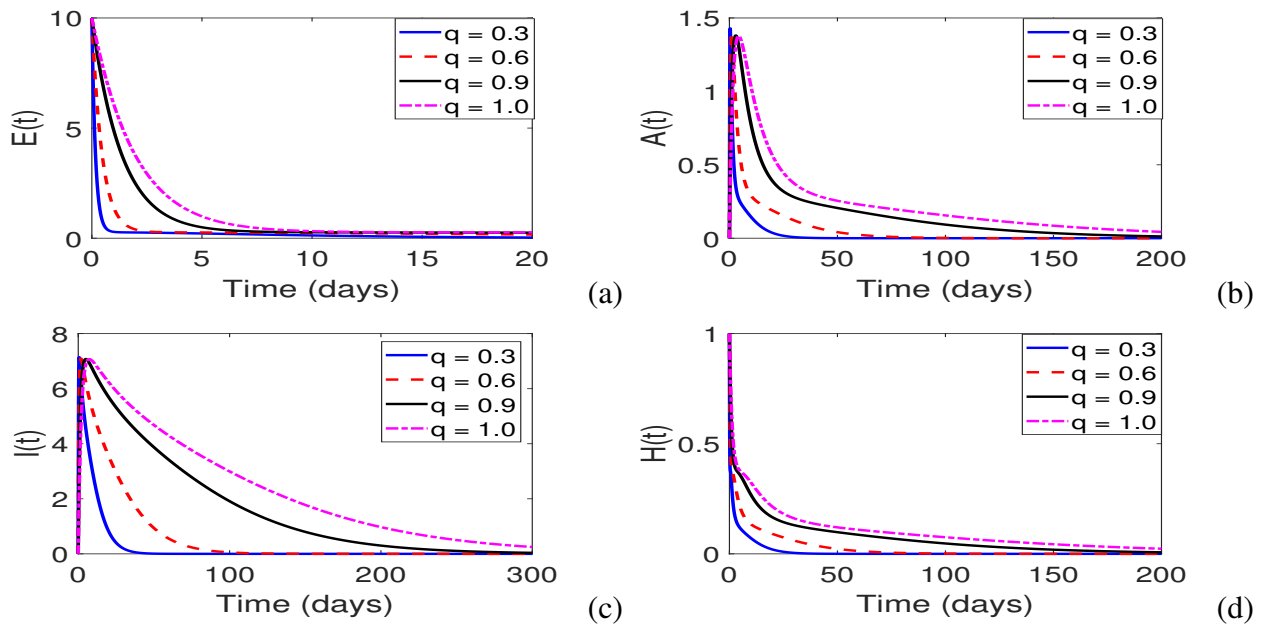


Figure 9. Simulation results showing convergence of solutions to the disease-free equilibrium whenever $\mathcal{R}_0 < 1$.

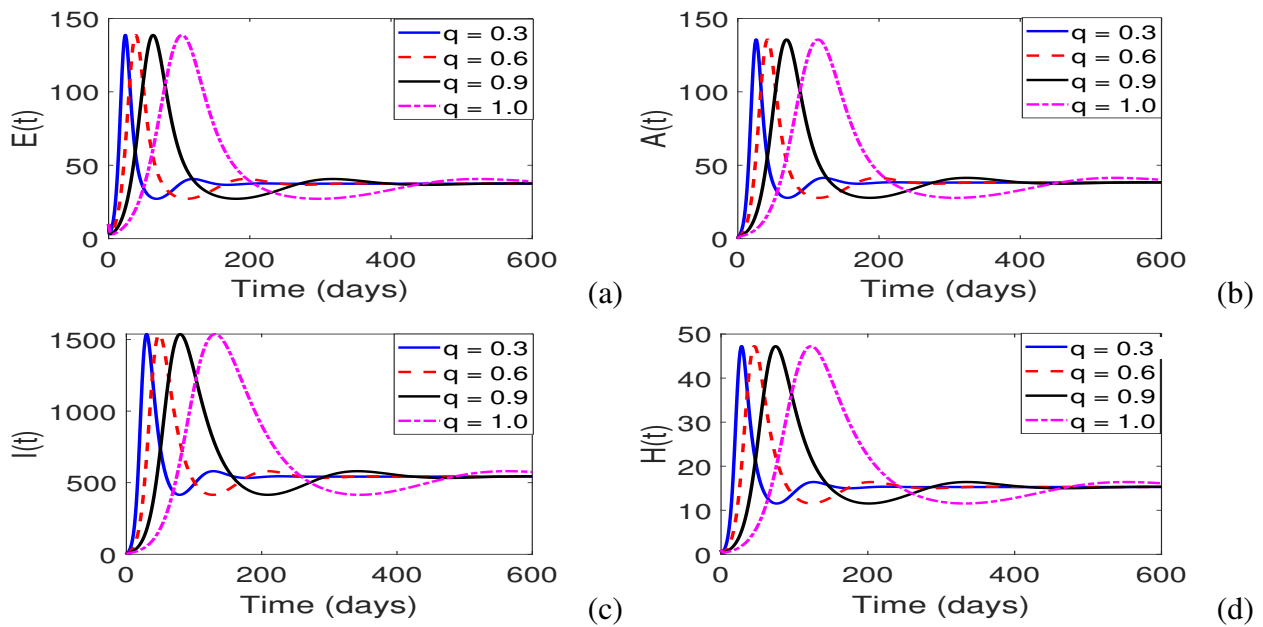


Figure 10. Convergence of model solutions to a unique endemic equilibrium whenever $\mathcal{R}_0 > 1$.

4. Conclusion remarks

Mathematical models are invaluable tools that can be used to quantitatively evaluate vaccination programs, improve their design and monitor new vaccine initiatives. Although vaccination is voluntary, the success attained by rolling out vaccines lies on vaccine efficacy and its acceptance by the target population. With the efficacy of COVID-19 vaccines estimated to be in the range of 50–95% efficacy [31], their success essentially depended on their acceptance by the population. Despite being highly effective, COVID-19 roll-out has been characterized by vaccine hesitancy. Globally, vaccine hesitancy and objection has been estimated to be around 27% [13]. Using a fractional model in this paper, we evaluated the vaccine hesitancy on COVID-19 dynamics over time. In particular, we evaluated the effects of delaying the first and second COVID-19 dose on disease dynamics over time. In addition, the model also includes the effects of non-pharmaceutical interventions (NPIs).

We employed a fractional model since model based on fractional calculus are capable of describing real world phenomena more accurately compared to integer ordinary differential equations. In particular, we used the Caputo derivative since its derivative for a constant has the same outcome as that of an integer ordinary differential equation. We computed the reproduction number and carried out sensitivity analysis using the partial rank correlation method to assess its relationship with model parameters. Sensitivity analysis results showed that vaccines with relatively high efficacy are capable of minimizing the spread of the epidemic. We also observed that reducing the delay to accept the first and second vaccine doses significantly reduces the epidemic outcomes. In contrast, we observe that parameters associated with recruitment rate of the population and disease transmission can significantly increase the epidemic whenever they are increased.

We also examined the global stability of the model steady states. By constructing suitable Lyapunov functionals, we demonstrated the both the disease-free and endemic equilibrium are globally asymptotically stable whenever they exist. The aforementioned analytical results are supported by numerical illustrations. To underpin and demonstrate this study, we carried out extensive numerical simulations, in particular, we assessed the effects of NPIs and vaccination on disease dynamics. Results showed that vaccines and NPIs interventions that are 75% effective all the time are capable of stopping the epidemic. We also evaluated the implications of vaccine hesitancy on disease dynamics. Outcomes showed that delaying accepting COVID-19 vaccines have public health implications. In particular, a delay of more than 10 and 100 days for the first and second dose, respectively, leads to disease persistence.

Our study has limitations. First, vaccine hesitancy can be triggered or aided by proliferation of anti-vaccination misinformation through social media [32]. As a future work, it will be interesting to modify the proposed model to incorporate media effects. Second, we did not account for heterogeneity in disease transmission. Risks of acquisition, spread, clinical symptoms and disease severity are heterogeneous, as are access to and uptake of universal strategies of confinement, testing and isolation [33]. Despite all these limitations, our findings might be useful for designing and implementing vaccination programs.

5. Supplement

5.1. Supplement A: Existence, uniqueness, positivity and boundedness of model solutions

In this section, we present the existence, uniqueness, positivity and boundedness of the solutions of model (2.2). We commence our discussion by demonstrating existence and uniqueness of solutions. Our approach is based on the fixed-point theory. Let \mathcal{B} be a Banach space of real-valued continuous functions defined on an interval \mathcal{I} with the associated norm:

$$\|S, V, E, A, I, H, R\| = \|S\| + \|V\| + \|E\| + \|A\| + \|I\| + \|H\| + \|R\| \quad (5.1)$$

where $\|S\| = \sup\{|S(t)| : t \in \mathcal{I}\}$, $\|V\| = \sup\{|V(t)| : t \in \mathcal{I}\}$, $\|E\| = \sup\{|E(t)| : t \in \mathcal{I}\}$, $\|A\| = \sup\{|A(t)| : t \in \mathcal{I}\}$, $\|I\| = \sup\{|I(t)| : t \in \mathcal{I}\}$, $\|H\| = \sup\{|H(t)| : t \in \mathcal{I}\}$, $\|R\| = \sup\{|R(t)| : t \in \mathcal{I}\}$, and $\mathcal{B} = \mathcal{E}(\mathcal{I}) \times \mathcal{E}(\mathcal{I}) \times \mathcal{E}(\mathcal{I}) \times \mathcal{E}(\mathcal{I}) \times \mathcal{E}(\mathcal{I}) \times \mathcal{E}(\mathcal{I}) \times \mathcal{E}(\mathcal{I})$, with $\mathcal{E}(\mathcal{I})$ denoting the Banach space of real-valued continuous functions on \mathcal{I} and the associated sup norm. For convenience system (2.2) can be rewritten in the equivalent form given below

$$\left. \begin{aligned} D_{t_0}^q S(t) &= G_1(t, S), \\ D_{t_0}^q V(t) &= G_2(t, V), \\ D_{t_0}^q E(t) &= G_3(t, E), \\ D_{t_0}^q A(t) &= G_4(t, A), \\ D_{t_0}^q I(t) &= G_5(t, I), \\ D_{t_0}^q H(t) &= G_6(t, H), \\ D_{t_0}^q R(t) &= G_7(t, R). \end{aligned} \right\} \quad (5.2)$$

By applying the Caputo fractional integral operator, system (5.2), reduces to the following integral equation of Volterra type with Caputo fractional integral of order $0 < q < 1$,

$$\left. \begin{aligned} S(t) - S(0) &= \frac{1}{\Gamma(q)} \int_0^t (t - \chi)^{q-1} G_1(\chi, S) d\chi, \\ V(t) - V(0) &= \frac{1}{\Gamma(q)} \int_0^t (t - \chi)^{q-1} G_2(\chi, V) d\chi, \\ E(t) - E(0) &= \frac{1}{\Gamma(q)} \int_0^t (t - \chi)^{q-1} G_3(\chi, E) d\chi, \\ A(t) - A(0) &= \frac{1}{\Gamma(q)} \int_0^t (t - \chi)^{q-1} G_4(\chi, A) d\chi, \\ I(t) - I(0) &= \frac{1}{\Gamma(q)} \int_0^t (t - \chi)^{q-1} G_5(\chi, I) d\chi, \\ H(t) - H(0) &= \frac{1}{\Gamma(q)} \int_0^t (t - \chi)^{q-1} G_6(\chi, H) d\chi, \\ R(t) - R(0) &= \frac{1}{\Gamma(q)} \int_0^t (t - \chi)^{q-1} G_7(\chi, R) d\chi. \end{aligned} \right\} \quad (5.3)$$

Next we prove that the kernels G_i , $i = 1, 2, 3, 4, 5, 6, 7$ fulfill the Lipschitz condition and contraction under some assumptions. In the following theorem, we have demonstrated for G_1 and one can easily verify for the remainder.

Theorem 5.1. *Let us consider the following inequality*

$$0 \leq (\beta(1 - \epsilon)(k_1 + k_2 + k_3) + \mu + \kappa) < 1.$$

The kernel G_1 satisfies the Lipschitz condition as well as contraction if the above inequality is satisfied.

Proof. For S and S_1 we proceed as below.

$$\begin{aligned} \|G_1(t, S) - G_1(t, S_1)\| &= \| -(\beta(1 - \epsilon)(H + A + I) + \mu + \kappa)(S(t) - S_1(t)) \\ &= (\mu + \kappa)\|S - S_1\| + \beta(1 - \epsilon)\|(A + I + H)(S - S_1)\|. \end{aligned} \quad (5.4)$$

Since $A(t)$, $I(t)$ and $H(t)$ are bounded functions, i.e., $\|A\| \leq k_1$, $\|I\| \leq k_2$ and $\|H\| \leq k_3$, by the property of norm functions, the above inequality (5.4) can be written as

$$\|G_1(t, S) - G_1(t, S_1)\| \leq \eta_1\|S(t) - S_1(t)\|, \quad (5.5)$$

where $\eta_1 = \beta(1 - \epsilon)(k_1 + k_2 + k_3) + \mu + \kappa$. Hence for G_1 the Lipschitz condition is obtained and if an additionally $0 \leq \beta(1 - \epsilon)(k_1 + k_2 + k_3) + \mu + \kappa < 1$, we obtain a contraction. The Lipschitz condition for the other kernels are

$$\left. \begin{aligned} \|G_2(t, V) - G_2(t, V_1)\| &\leq \eta_2\|V(t) - V_1(t)\|, \\ \|G_3(t, E) - G_3(t, E_1)\| &\leq \eta_3\|E(t) - E_1(t)\|, \\ \|G_4(t, A) - G_4(t, A_1)\| &\leq \eta_4\|A(t) - A_1(t)\|, \\ \|G_5(t, I) - G_5(t, I_1)\| &\leq \eta_5\|I(t) - I_1(t)\|, \\ \|G_6(t, H) - G_6(t, H_1)\| &\leq \eta_6\|H(t) - H_1(t)\|, \\ \|G_7(t, R) - G_7(t, R_1)\| &\leq \eta_7\|R(t) - R_1(t)\|. \end{aligned} \right\} \quad (5.6)$$

□

Recursively, the expression in (5.3) can be written as

$$\left. \begin{aligned} S_n(t) - S(0) &= \frac{1}{\Gamma(q)} \int_0^t (t - \chi)^{q-1} G_1(\chi, S_{n-1}) d\chi, \\ V_n(t) - V(0) &= \frac{1}{\Gamma(q)} \int_0^t (t - \chi)^{q-1} G_2(\chi, V_{n-1}) d\chi, \\ E_n(t) - E(0) &= \frac{1}{\Gamma(q)} \int_0^t (t - \chi)^{q-1} G_3(\chi, E_{n-1}) d\chi, \\ A_n(t) - A(0) &= \frac{1}{\Gamma(q)} \int_0^t (t - \chi)^{q-1} G_4(\chi, A_{n-1}) d\chi, \\ I_n(t) - I(0) &= \frac{1}{\Gamma(q)} \int_0^t (t - \chi)^{q-1} G_5(\chi, I_{n-1}) d\chi, \\ H_n(t) - H(0) &= \frac{1}{\Gamma(q)} \int_0^t (t - \chi)^{q-1} G_6(\chi, H_{n-1}) d\chi, \\ R_n(t) - R(0) &= \frac{1}{\Gamma(q)} \int_0^t (t - \chi)^{q-1} G_7(\chi, R_{n-1}) d\chi. \end{aligned} \right\} \quad (5.7)$$

The difference between successive terms of system (5.2) in recursive form is given below:

$$\left. \begin{aligned}
 \phi_{1n} &= S_n(t) - S_{n-1}(t) \\
 &= \frac{1}{\Gamma(q)} \int_0^t (t-\chi)^{q-1} (G_1(\chi, S_{n-1}) - G_1(\chi, S_{n-2})) d\chi, \\
 \phi_{2n} &= V_n(t) - V_{n-1}(t) \\
 &= \frac{1}{\Gamma(q)} \int_0^t (t-\chi)^{q-1} (G_2(\chi, V_{n-1}) - G_2(\chi, V_{n-2})) d\chi, \\
 \phi_{3n} &= E_n(t) - E_{n-1}(t) \\
 &= \frac{1}{\Gamma(q)} \int_0^t (t-\chi)^{q-1} (G_3(\chi, E_{n-1}) - G_3(\chi, E_{n-2})) d\chi, \\
 \phi_{4n} &= A_n(t) - A_{n-1}(t) \\
 &= \frac{1}{\Gamma(q)} \int_0^t (t-\chi)^{q-1} (G_4(\chi, A_{n-1}) - G_4(\chi, A_{n-2})) d\chi, \\
 \phi_{5n} &= I_n(t) - I_{n-1}(t) \\
 &= \frac{1}{\Gamma(q)} \int_0^t (t-\chi)^{q-1} (G_5(\chi, I_{n-1}) - G_5(\chi, I_{n-2})) d\chi, \\
 \phi_{6n} &= H_n(t) - H_{n-1}(t) \\
 &= \frac{1}{\Gamma(q)} \int_0^t (t-\chi)^{q-1} (G_6(\chi, H_{n-1}) - G_6(\chi, H_{n-2})) d\chi, \\
 \phi_{7n} &= R_n(t) - R_{n-1}(t) \\
 &= \frac{1}{\Gamma(q)} \int_0^t (t-\chi)^{q-1} (G_7(\chi, R_{n-1}) - G_7(\chi, R_{n-2})) d\chi,
 \end{aligned} \right\} \quad (5.8)$$

with the initial conditions $S_0(t) = S(0)$, $V_0(t) = V(0)$, $E_0(t) = E$, $A_0(t) = A(0)$, $H_0(t) = H(0)$ and $R_0(t) = R_0$. Taking the norm of the first equation of (5.8), we obtain

$$\begin{aligned}
 \|\phi_{1n}(t)\| &= \|S_n(t) - S_{n-1}(t)\| \\
 &= \left\| \frac{1}{\Gamma(q)} \int_0^t (t-\chi)^{q-1} (G_1(\chi, S_{n-1}) - G_1(\chi, S_{n-2})) d\chi \right\| \\
 &\leq \frac{1}{\Gamma(q)} \left\| \int_0^t (t-\chi)^{q-1} (G_1(\chi, S_{n-1}) - G_1(\chi, S_{n-2})) d\chi \right\|.
 \end{aligned} \quad (5.9)$$

Applying the Lipschitz condition (5.5) one gets

$$\|S_n(t) - S_{n-1}(t)\| \leq \frac{1}{\Gamma(q)} \eta_1 \int_0^t (t-\chi)^{q-1} \|S_{n-1} - S_{n-2}\| d\chi. \quad (5.10)$$

Thus, we have

$$\|\phi_{1n}(t)\| \leq \frac{1}{\Gamma(q)} \eta_1 \int_0^t (t-\chi)^{q-1} \|\phi_{1n}(t)\| d\chi. \quad (5.11)$$

Similarly, for the remainder of the equations in system (2.2) we have

$$\left. \begin{aligned}
 \|\phi_{2n}(t)\| &\leq \frac{1}{\Gamma(q)} \eta_2 \int_0^t (t-\chi)^{q-1} \|\phi_{2n}(t)\| d\chi, \\
 \|\phi_{3n}(t)\| &\leq \frac{1}{\Gamma(q)} \eta_3 \int_0^t (t-\chi)^{q-1} \|\phi_{3n}(t)\| d\chi, \\
 \|\phi_{4n}(t)\| &\leq \frac{1}{\Gamma(q)} \eta_4 \int_0^t (t-\chi)^{q-1} \|\phi_{4n}(t)\| d\chi, \\
 \|\phi_{5n}(t)\| &\leq \frac{1}{\Gamma(q)} \eta_5 \int_0^t (t-\chi)^{q-1} \|\phi_{5n}(t)\| d\chi, \\
 \|\phi_{6n}(t)\| &\leq \frac{1}{\Gamma(q)} \eta_6 \int_0^t (t-\chi)^{q-1} \|\phi_{6n}(t)\| d\chi, \\
 \|\phi_{7n}(t)\| &\leq \frac{1}{\Gamma(q)} \eta_7 \int_0^t (t-\chi)^{q-1} \|\phi_{7n}(t)\| d\chi.
 \end{aligned} \right\} \quad (5.12)$$

From (5.12) one can write

$$\left. \begin{aligned} S_n(t) &= \sum_{i=1}^n \phi_{1i}(t), & V_n(t) &= \sum_{i=1}^n \phi_{2i}(t), & E_n(t) &= \sum_{i=1}^n \phi_{3i}(t), \\ A_n(t) &= \sum_{i=1}^n \phi_{4i}(t), & I_n(t) &= \sum_{i=1}^n \phi_{5i}(t), & H_n(t) &= \sum_{i=1}^n \phi_{6i}(t), \\ R_n(t) &= \sum_{i=1}^n \phi_{7i}(t), \end{aligned} \right\} \quad (5.13)$$

Now, we claim the following result which guaranteed the uniqueness of solution of model (2.2).

Theorem 5.2. *The proposed fractional epidemic model (2.2) has a unique solution for $t \in [0, T]$ if the following inequality holds*

$$\frac{1}{\Gamma(q)} b^q \eta_i < 1, \quad i = 1, 2, \dots, 7. \quad (5.14)$$

Proof. Earlier we have shown that the kernels conditions given in Eqs. (5.5) and (5.6) holds. Thus by considering the Eqs. (5.12) and (5.14), and by applying the recursive technique we obtained the succeeding results as below

$$\left. \begin{aligned} \|\phi_{1n}(t)\| &\leq \|S_0(t)\| \left[\frac{1}{\Gamma(q)} b^q \eta_1 \right]^n, & \|\phi_{2n}(t)\| &\leq \|V_0(t)\| \left[\frac{1}{\Gamma(q)} b^q \eta_2 \right]^n, & \|\phi_{3n}(t)\| &\leq \|E_0(t)\| \left[\frac{1}{\Gamma(q)} b^q \eta_3 \right]^n, \\ \|\phi_{4n}(t)\| &\leq \|A_0(t)\| \left[\frac{1}{\Gamma(q)} b^q \eta_4 \right]^n, & \|\phi_{5n}(t)\| &\leq \|I_0(t)\| \left[\frac{1}{\Gamma(q)} b^q \eta_5 \right]^n, & \|\phi_{6n}(t)\| &\leq \|H_0(t)\| \left[\frac{1}{\Gamma(q)} b^q \eta_6 \right]^n, \\ \|\phi_{7n}(t)\| &\leq \|R_0(t)\| \left[\frac{1}{\Gamma(q)} b^q \eta_7 \right]^n. \end{aligned} \right\} \quad (5.15)$$

Therefore, the above mentioned sequences exist and satisfy $\|\phi_{1n}(t)\| \rightarrow 0, \|\phi_{2n}(t)\| \rightarrow 0, \|\phi_{3n}(t)\| \rightarrow 0, \|\phi_{4n}(t)\| \rightarrow 0, \|\phi_{5n}(t)\| \rightarrow 0, \|\phi_{6n}(t)\| \rightarrow 0,$ and $\|\phi_{7n}(t)\| \rightarrow 0,$ as $n \rightarrow \infty.$ Furthermore, from Eq. (5.15) and employing the triangle inequality for any $k,$ we one gets

$$\left. \begin{aligned} \|S_{n+k}(t) - S_n(t)\| &\leq \sum_{j=n+1}^{n+k} T_1^j = \frac{T_1^{n+1} - T_1^{n+k+1}}{1 - T_1}, \\ \|V_{n+k}(t) - V_n(t)\| &\leq \sum_{j=n+1}^{n+k} T_2^j = \frac{T_2^{n+1} - T_2^{n+k+1}}{1 - T_2}, \\ \|E_{n+k}(t) - E_n(t)\| &\leq \sum_{j=n+1}^{n+k} T_3^j = \frac{T_3^{n+1} - T_3^{n+k+1}}{1 - T_3}, \\ \|A_{n+k}(t) - A_n(t)\| &\leq \sum_{j=n+1}^{n+k} T_4^j = \frac{T_4^{n+1} - T_4^{n+k+1}}{1 - T_4}, \\ \|I_{n+k}(t) - I_n(t)\| &\leq \sum_{j=n+1}^{n+k} T_5^j = \frac{T_5^{n+1} - T_5^{n+k+1}}{1 - T_5}, \\ \|H_{n+k}(t) - H_n(t)\| &\leq \sum_{j=n+1}^{n+k} T_6^j = \frac{T_6^{n+1} - T_6^{n+k+1}}{1 - T_6}, \\ \|R_{n+k}(t) - R_n(t)\| &\leq \sum_{j=n+1}^{n+k} T_7^j = \frac{T_7^{n+1} - T_7^{n+k+1}}{1 - T_7}, \end{aligned} \right\} \quad (5.16)$$

where $T_i = \frac{1}{\Gamma(q)} b^q \eta_i < 1$ by hypothesis. Therefore, S_n, E_n, A_n, I_n, H_n and R_n are regarded as Cauchy sequences in the Banach space $B(J)$. Hence they are uniformly convergent as described in [34]. Applying the limit theory on Eq. (5.7) when $n \rightarrow \infty$ affirms that the limit of these sequences is the unique solution of system (2.2). Ultimately, the existence of a unique solution for system (2.2) has been achieved. \square

We now demonstrate the positivity of solutions for all $t \geq 0$. To prove positivity and boundedness of solutions, we need the following Generalized Mean Value Theorem in [35] and corollary.

Lemma 5.1. *Suppose that $f(x) \in C[a, b]$ and $D_{t_0}^q f(x) \in C[a, b]$, for $0 < q \leq 1$, then we have*

$$f(x) = f(a) + \frac{1}{\Gamma(q)} (D_{t_0}^q f)(\xi)(x - a)^q \quad (5.17)$$

with $a \leq \xi x, \forall x \in (a, b]$ and $\Gamma(\cdot)$ is the gamma function.

Corollary 5.1. *Suppose that $f(x) \in C[a, b]$ and $D_{t_0}^q f(x) \in C(a, b]$, for $0 < q \leq 1$. If $D_{t_0}^q f(x) \geq 0, \forall x \in (a, b)$, then $f(x)$ is non-decreasing for each $x \in [a, b]$. If $D_{t_0}^q f(x) \leq 0, \forall x \in (a, b)$, then $f(x)$ is non-increasing for each $x \in [a, b]$.*

We now prove that the non-negative orthant \mathbb{R}_+^7 is positively invariant region. To do this, we need to show that on each hyperplane bounding the non-negative orthant, the vector field points to \mathbb{R}_+^7 . From model (2.2), one gets:

$$D_{t_0}^q S(t)|_{S=0} = \Lambda^q \geq 0, \quad (5.18)$$

$$D_{t_0}^q V(t)|_{V=0} = \kappa^q S \geq 0, \quad (5.19)$$

$$D_{t_0}^q E(t)|_{E=0} = \beta^q (1 - \epsilon)(H + A + I)(S + (1 - \phi)V) \geq 0, \quad (5.20)$$

$$D_{t_0}^q I(t)|_{I=0} = (1 - \omega)\alpha^q E \geq 0, \quad (5.21)$$

$$D_{t_0}^q A(t)|_{A=0} = \omega\alpha^q E \geq 0, \quad (5.22)$$

$$D_{t_0}^q H(t)|_{H=0} = \delta_2^q A + \delta_1^q I \geq 0, \quad (5.23)$$

$$D_{t_0}^q R(t)|_{R=0} = \gamma_1^q A + \gamma_2^q I + \gamma_3^q H + \theta_2^q V \geq 0. \quad (5.24)$$

Thus, by Corollary 5.1, the solution of model (2.2) are always positive for $t \geq 0$. We now demonstrate that all solutions of model (2.2) are bounded above for all $t \geq 0$. To do this, we need the following Lemma 5.2 and Lemma 5.3.

Lemma 5.2. (see [36]). *Let $q > 0, n - 1 < q < n - \mathbb{N}$. Suppose that $f(t), f'(t), \dots, f^{(n-1)}(t)$ are continuous on $[t_0, \infty)$ and the exponential order and that $D_{t_0}^q f(t)$ is piecewise continuous on $[t_0, \infty)$. Then*

$$\mathcal{L}\{D_{t_0}^q f(t)\} = s^q \mathcal{F}(s) - \sum_{k=0}^{n-1} s^{q-k-1} f^{(k)}(t_0) \quad (5.25)$$

where $\mathcal{F}(s) = \mathcal{L}\{f(t)\}$.

Lemma 5.3. (see [37]). *Let \mathbb{C} be the complex plane. For any $\alpha > 0, \beta > 0$, and $A \in \mathbb{C}^{n \times n}$, we have*

$$\mathcal{L}\{t^{\beta-1} E_{\alpha, \beta}(At^\alpha)\} = s^{\alpha-\beta} (s^\alpha - A)^{-1},$$

for $\Re s > \|A\|^\frac{1}{\alpha}$, where $\Re s$ represents the real part of the complex number s , and $E_{\alpha, \beta}$ is the Mittag-Leffler function [21].

Since all solutions of model system (2.2) have been shown to be positively invariant and have a lower bound zero (5.18)-(5.24), we now proceed to demonstrate that these solutions are bounded above. By summing all equations of system (2.2) one gets:

$$\begin{aligned} D_{t_0}^q N(t) &= \Lambda^q - \mu^q N(t) - d^q I(t) - d^q H(t) \\ &\leq \Lambda^q - \mu^q N(t). \end{aligned} \quad (5.26)$$

Taking the Laplace transform of (5.26) leads to:

$$s^q \mathcal{L}(N(t)) - s^{q-1} N(0) \leq \frac{\Lambda^q}{s} - \mu^q \mathcal{L}(N(t)). \quad (5.27)$$

Combining like terms and arranging leads to

$$\begin{aligned} \mathcal{L}(N(t)) &\leq \Lambda^q \frac{s^{-1}}{s^q + \mu^q} + N(0) \frac{s^{q-1}}{s^q + \mu^q} \\ &= \Lambda^q \frac{s^{q-(1+q)}}{s^q + \mu^q} + N(0) \frac{s^{q-1}}{s^q + \mu^q}. \end{aligned} \quad (5.28)$$

Applying the inverse Laplace transform leads to

$$\begin{aligned} N(t) &\leq \mathcal{L}^{-1} \left\{ \Lambda^q \frac{s^{-1}}{s^q + \mu^q} + N(0) \frac{s^{q-1}}{s^q + \mu^q} \right\} + \mathcal{L}^{-1} \left\{ N(0) \frac{s^{q-1}}{s^q + \mu^q} \right\} \\ &\leq \Lambda^q t^q E_{q,q+1}(-\mu t^q) + N(0) E_{q,1}(-\mu t^q) \\ &\leq \frac{\Lambda^q}{\mu^q} \mu^q t^q E_{q,q+1}(-\mu t^q) + N(0) E_{q,1}(-\mu t^q) \\ &\leq \max \left\{ \frac{\Lambda^q}{\mu^q}, N(0) \right\} (\mu^q t^q E_{q,q+1}(-\mu t^q) + E_{q,1}(-\mu t^q)) \\ &= \frac{C}{\Gamma(1)} = C, \end{aligned} \quad (5.29)$$

where $C = \max \left\{ \frac{\Lambda^q}{\mu^q}, N(0) \right\}$. Thus, $N(t)$ is bounded from above. This completes the proof of Theorem 3.1.

5.2. Supplement B: Reproduction number

In order to compute the reproduction number using the next generation matrix (NGM) method [24] we first evaluate the disease-free equilibrium (DFE). Through direct calculations one can easily verify that in the absence of COVID-19 in the community the DFE of model (2.2) is:

$$\mathcal{E}^0 : (S^0, V^0, E^0, A^0, I^0, H^0, R^0) = \left(\frac{\Lambda^q}{\mu^q + \kappa^q}, \frac{\kappa^q \Lambda^q}{(\kappa^q + \mu^q)(\mu^q + \theta_2^q)}, 0, 0, 0, 0, 0 \right). \quad (5.30)$$

We now define the nonnegative matrix \mathcal{F} that denotes the generation of new infection terms and the non-singular matrix \mathcal{V} that denotes the remaining transfer terms are respectively given (at the disease-

free equilibrium \mathcal{E}^0) by:

$$\mathcal{F} = \beta^q(1-\epsilon)(S^0 + (1-\phi)V^0) \begin{bmatrix} 1 & 1 & 1 & 1 \\ 0 & 0 & 0 & 0 \\ 0 & 0 & 0 & 0 \\ 0 & 0 & 0 & 0 \end{bmatrix},$$

$$\mathcal{V} = \begin{bmatrix} \alpha^q + \mu^q & 0 & 0 & 0 \\ -(1-\omega)\alpha^q & \mu^q + \gamma_1^q + \delta_2^q & 0 & 0 \\ -\omega\alpha^q & 0 & \mu^q + d^q + \gamma_2^q + \delta_1^q & 0 \\ 0 & -\delta_2^q & -\delta_1^q & \mu^q + d^q + \gamma_3^q \end{bmatrix}. \quad (5.31)$$

It follows from (5.31), that the NGM \mathbf{K} of the model (2.2) is (5.32)

$$\mathbf{K} = \begin{bmatrix} m_1 & m_2 & m_3 & m_4 \\ 0 & 0 & 0 & 0 \\ 0 & 0 & 0 & 0 \\ 0 & 0 & 0 & 0 \end{bmatrix}, \quad (5.32)$$

where

$$m_1 = \frac{\beta^q(1-\epsilon)(1-\omega)}{(\alpha^q + \mu^q)(\mu^q + \gamma_1^q + \delta_2^q)} \left(\frac{\Lambda^q}{\mu^q + \kappa^q} + \frac{\kappa^q(1-\phi)\Lambda^q}{(\kappa^q + \mu^q)(\mu^q + \theta_2^q)} \right) \left(\alpha^q + \frac{\delta_2^q}{\mu^q + d^q + \gamma_3^q} \right) + \frac{\beta^q(1-\epsilon)\omega}{(\alpha^q + \mu^q)(\mu^q + d^q + \gamma_2^q + \delta_1^q)} \left(\frac{\Lambda^q}{\mu^q + \kappa^q} + \frac{\kappa^q(1-\phi)\Lambda^q}{(\kappa^q + \mu^q)(\mu^q + \theta_2^q)} \right) \left(\alpha^q + \frac{\delta_1^q}{\mu^q + d^q + \gamma_3^q} \right), \quad (5.33)$$

$$m_2 = \frac{\beta^q(1-\epsilon)}{(\mu^q + \gamma_1^q + \delta_2^q)} \left(\frac{\Lambda^q}{\mu^q + \kappa^q} + \frac{\kappa^q(1-\phi)\Lambda^q}{(\kappa^q + \mu^q)(\mu^q + \theta_2^q)} \right) \left(1 + \frac{\delta_2^q}{\mu^q + d^q + \gamma_3^q} \right), \quad (5.34)$$

$$m_3 = \frac{\beta^q(1-\epsilon)}{(\mu^q + d^q + \gamma_2^q + \delta_1^q)} \left(\frac{\Lambda^q}{\mu^q + \kappa^q} + \frac{\kappa^q(1-\phi)\Lambda^q}{(\kappa^q + \mu^q)(\mu^q + \theta_2^q)} \right) \left(1 + \frac{\delta_1^q}{\mu^q + d^q + \gamma_3^q} \right), \quad (5.35)$$

$$m_4 = \frac{\beta^q(1-\epsilon)}{(\mu^q + d^q + \gamma_3^q)} \left(\frac{\Lambda^q}{\mu^q + \kappa^q} + \frac{\kappa^q(1-\phi)\Lambda^q}{(\kappa^q + \mu^q)(\mu^q + \theta_2^q)} \right). \quad (5.36)$$

The spectral radius of (5.32) gives the reproduction number of model (2.2) is given by Equation (3.2).

5.3. Supplement C: Stability of the model steady states

To investigate the global stability of the model steady states we will construct appropriate Lyapunov functionals. Since the recovered/removed population does not contribute to the generation of secondary infections one can ignore that last equation of model (2.2) when examining the global stability and consider the following reduced system

$$\left. \begin{aligned} D_{t_0}^q S(t) &= \Lambda^q - \beta^q(1-\epsilon)(H + A + I)S - (\mu^q + \kappa^q)S, \\ D_{t_0}^q V(t) &= \kappa^q S - \beta^q(1-\phi)(1-\epsilon)(H + A + I)V - (\mu^q + \theta_2^q)V, \\ D_{t_0}^q E(t) &= \beta^q(1-\epsilon)(H + A + I)(S + (1-\phi)V) - (\alpha^q + \mu^q)E, \\ D_{t_0}^q I(t) &= \omega\alpha^q E - (\mu^q + d + \gamma_2^q + \delta_1^q)I, \\ D_{t_0}^q A(t) &= (1-\omega)\alpha^q E - (\mu^q + \gamma_1^q + \delta_2^q)A, \\ D_{t_0}^q H(t) &= \delta_1^q I + \delta_2^q A - (\mu^q + d^q + \gamma_3^q)H. \end{aligned} \right\} \quad (5.37)$$

Now, to investigate the global stability of the DFE let us consider the Lyapunov functional (5.38):

$$\mathcal{L}_0(t) = a_1 E(t) + a_2 I(t) + a_3 A(t) + a_4 H(t), \quad (5.38)$$

where

$$\begin{aligned} a_1 &= \frac{\beta\omega\alpha}{\hbar_1\hbar_2} + \frac{\beta(1-\omega)\alpha}{\hbar_1\hbar_3} + \frac{\beta\omega\alpha\delta_1}{\hbar_1\hbar_2\hbar_4} + \frac{\beta(1-\omega)\alpha\delta_2}{\hbar_1\hbar_3\hbar_4}, \\ a_2 &= \frac{\beta}{\hbar_2} + \frac{\beta\delta_1}{\hbar_2\hbar_4}, \quad a_3 = \frac{\beta}{\hbar_3} + \frac{\beta\delta_2}{\hbar_3\hbar_4}, \quad a_4 = \frac{\beta}{\hbar_4}, \end{aligned}$$

where,

$$\hbar_1 = (\mu + \alpha), \quad \hbar_2 = (\mu + d + \gamma_2 + \delta_1), \quad \hbar_3 = (\mu + \gamma_1 + \delta_2), \quad \hbar_4 = (\mu + d + \gamma_3).$$

Taking the derivative of $\mathcal{L}_0(t)$ along the solutions system (5.37) and making some algebraic simplification lead one gets:

$$\mathcal{L}'_0(t) \leq \beta(1-\epsilon)(\mathcal{R}_0 - 1)(I(t) + A(t) + H(t)). \quad (5.39)$$

If $\mathcal{R}_0 \leq 1$, then $\mathcal{L}'_0(t) \leq 0$. Let M be the largest invariant set in Ω , we can observe that $\mathcal{L}'_0(t) = 0$ iff either $\mathcal{R}_0 = 1$. Therefore, by the Lyapunov-LaSalle invariance principle [38], the DFE is globally asymptotically stable whenever $\mathcal{R}_0 \leq 1$. This completes the proof.

To demonstrate the second part of Theorem 3.2, we need Lemma 5.4 in [39]:

Lemma 5.4. *Let $x(\cdot)$ be a continuous and differentiable function with $x(t) \in \mathbb{R}_+$. Then, for any time instant $t \geq b$, one has*

$${}_b^c D_t^q \left(x(t) - x^* - x^* \ln \frac{x(t)}{x^*} \right) \leq \left(1 - \frac{x^*}{x(t)} \right) {}_b^c D_t^q x(t), \quad x^* \in \mathbb{R}^+, \quad \forall q \in (0, 1). \quad (5.40)$$

We now proceed to investigate the global stability of the endemic equilibrium. We define the Lyapunov functional:

$$\begin{aligned} \mathcal{W}(t) &= B_1 \left\{ S - S^* - S^* \ln \left(\frac{S}{S^*} \right) \right\} + B_2 \left\{ V - V^* - V^* \ln \left(\frac{V}{V^*} \right) \right\} + B_3 \left\{ E - E^* - E^* \ln \left(\frac{E}{E^*} \right) \right\} \\ &+ B_4 \left\{ A - A^* - A^* \ln \left(\frac{A}{A^*} \right) \right\} + B_5 \left\{ I - I^* - I^* \ln \left(\frac{I}{I^*} \right) \right\} + B_6 \left\{ H - H^* - H^* \ln \left(\frac{H}{H^*} \right) \right\}, \end{aligned} \quad (5.41)$$

with

$$\begin{aligned} B_1 &= B_2 = B_3 = 1, \\ B_4 &= \frac{\beta^q(1-\epsilon)A^*(S^* + (1-\phi)V^*)}{(1-\omega)\alpha^q E^*} + \frac{\beta^q(1-\epsilon)\delta_2^q A^* H^*}{(1-\omega)\alpha^q E^*} \left(\frac{S^* + (1-\phi)V^*}{\delta_2^q A^* + \delta_1^q I^*} \right), \\ B_5 &= \frac{\beta^q(1-\epsilon)I^*(S^* + (1-\phi)V^*)}{\omega\alpha^q E^*} + \frac{\beta^q(1-\epsilon)\delta_1^q I^* H^*}{\omega\alpha^q E^*} \left(\frac{S^* + (1-\phi)V^*}{\delta_2^q A^* + \delta_1^q I^*} \right), \end{aligned}$$

$$B_6 = \frac{\beta^q(1-\epsilon)H^*(S^* + (1-\phi)V^*)}{\delta_2^q A^* + \delta_1^q I^*}. \quad (5.42)$$

Applying Lemma 5.4 leads to (5.43):

$$\begin{aligned} D_{t_0}^q \mathcal{W}(t) \leq & (\mu^q + \kappa^q)S^* \left(2 - x_1 - \frac{1}{x_1}\right) + (\mu^q + \theta_2^q)V^* \left(3 - \frac{x_1}{x_2} - \frac{1}{x_1} - x_2\right) \\ & + \beta^q(1-\epsilon)A^*S^* \left(3 - \frac{1}{x_1} - \frac{x_3}{x_4} - \frac{x_4}{x_3}x_1\right) + \beta^q(1-\epsilon)I^*S^* \left(3 - \frac{1}{x_1} - \frac{x_3}{x_5} - \frac{x_5}{x_3}x_1\right) \\ & + \frac{\beta^q(1-\epsilon)\delta_2^q A^* H^* S^*}{(\delta_2^q A^* + \delta_1^q I^*)} \left(4 - \frac{1}{x_1} - \frac{x_3}{x_4} - \frac{x_4}{x_6} - \frac{x_6}{x_3}x_1\right) \\ & + \beta^q(1-\epsilon)(1-\phi)A^*V^* \left(4 - \frac{1}{x_1} - \frac{x_1}{x_2} - \frac{x_3}{x_4} - \frac{x_4}{x_3}x_2\right) \\ & + \beta^q(1-\epsilon)(1-\phi)I^*V^* \left(4 - \frac{1}{x_1} - \frac{x_1}{x_2} - \frac{x_3}{x_5} - \frac{x_5}{x_3}x_2\right) \\ & + \frac{\beta^q(1-\epsilon)\delta_1^q I^* H^* S^*}{\delta_2^q A^* + \delta_1^q I^*} \left(4 - \frac{1}{x_1} - \frac{x_3}{x_5} - \frac{x_5}{x_6} - \frac{x_6}{x_3}x_1\right) \\ & + \frac{\beta^q(1-\epsilon)(1-\phi)\delta_2^q A^* H^* V^*}{(\delta_2^q A^* + \delta_1^q I^*)} \left(5 - \frac{1}{x_1} - \frac{x_1}{x_2} - \frac{x_3}{x_4} - \frac{x_4}{x_6} - \frac{x_6}{x_3}x_2\right) \\ & + \frac{\beta^q(1-\epsilon)(1-\phi)\delta_1^q I^* H^* V^*}{(\delta_2^q A^* + \delta_1^q I^*)} \left(5 - \frac{1}{x_1} - \frac{x_1}{x_2} - \frac{x_3}{x_5} - \frac{x_5}{x_6} - \frac{x_6}{x_3}x_2\right), \end{aligned} \quad (5.43)$$

where

$$x_1 = \frac{S}{S^*}, \quad x_2 = \frac{V}{V^*}, \quad x_3 = \frac{E}{E^*}, \quad x_4 = \frac{A}{A^*}, \quad x_5 = \frac{I}{I^*}, \quad x_6 = \frac{H}{H^*},$$

It follows that if $x_i = 1$, (for $i = 1, 2, 3, 4, 5$), that is., $S = S^*$, $V = V^*$, $E = E^*$, $A = A^*$, $I = I^*$ and $H = H^*$ one gets we have $D_{t_0}^q \mathcal{W}(t) = 0$. Furthermore, Since the arithmetic mean is greater or equal to the geometric mean, that is;

$$x_1 + \frac{1}{x_1} \geq 2 \sqrt{x_1 \cdot \frac{1}{x_1}},$$

it implies $D_{t_0}^q \mathcal{W}(t) \leq 0$. Using the LaSalle's invariance principle [38], we conclude that the endemic equilibrium point EE of model (2.2) is globally asymptotically stable if $\mathcal{R}_0 > 1$. This completes the second part of Theorem 3.2.

Acknowledgments

We are grateful to their respective institutions for the support they received while carrying out this study. In addition, we would like to thank the anonymous referees and the editors for their invaluable comments and suggestions.

Authors contributions

All authors have equal contributions and they read and approved the final version of the paper.

Use of AI tools declaration

The authors declare they have not used Artificial Intelligence (AI) tools in the creation of this article.

Conflict of interest

The authors declare that they have no conflicts of interest.

References

1. World Health Organization, Weekly epidemiological update on COVID-19—8 June 2023. World Health Organization, 2023. Available from: <https://www.who.int/publications/m/item/weekly-epidemiological-update-on-covid-19—8-june-2023>
2. Faiçal N, Iván A, Juan JN, et al. (2020) Mathematical modeling of COVID-19 transmission dynamics with a case study of Wuhan. *Chaos Solitons Fractals* 135: 109846. <https://doi.org/10.1016/j.chaos.2020.109846>
3. Rozenfeld Y, Beam J, Maier H, et al. (2020) A model of disparities: risk factors associated with COVID-19 infection. *Int J Equity Health* 19: 126. <https://doi.org/10.1186/s12939-020-01242-z>
4. Mushayabasa S, Ngarakana-Gwasira ET, Mushanyu J (2020) On the role of governmental action and individual reaction on COVID-19 dynamics in South Africa: A mathematical modelling study. *Inform Med Unlocked* 20: 100387. <https://doi.org/10.1016/j.imu.2020.100387>
5. Wang J, Chan YC, Niu R, et al. (2022) Modeling the impact of vaccination on COVID-19 and its Delta and Omicron variants. *Viruses* 14: 1482. <https://doi.org/10.3390/v14071482>
6. Ahmed I, Baba IA, Yusuf A, et al. (2020) Analysis of Caputo fractional-order model for COVID-19 with lockdown. *Adv Differ Equ* 2020: 394. <https://doi.org/10.1186/s13662-020-02853-0>
7. Khan T, Ullah R, Zaman G, et al. (2021) A mathematical model for the dynamics of SARS-CoV-2 virus using the Caputo-Fabrizio operator. *Math Biosci Eng* 18: 6095–6116. <https://doi.org/10.3934/mbe.2021305>
8. Ghosh I, Martcheva M (2021) Modeling the effects of prosocial awareness on COVID-19 dynamics: case studies on Colombia and India. *Nonlinear Dyn* 104: 4681–4700. <https://doi.org/10.1007/s11071-021-06489-x>

9. Omidvar Tehrani S, Perkins DD (2022) Public health resources, religion, and freedom as predictors of COVID-19 vaccination rates: A global study of 89 countries. *COVID 2*: 703–718. <https://doi.org/10.3390/covid2060053>
10. Oduro B, Miloua A, Apenteng OO, et al. (2021) COVID-19 vaccination hesitancy model: the impact of vaccine education on controlling the outbreak in the United States. *Math Model Appl 6*: 81–91. <https://doi.org/10.11648/j.mma.20210604.11>
11. Gravelle TB, Phillips JB, Reifler J, et al. (2022) Estimating the size of “anti-vax” and vaccine hesitant populations in the US, UK, and Canada: comparative latent class modeling of vaccine attitudes. *Hum Vaccin Immunother 18*: 2008214. <https://doi.org/10.1080/21645515.2021.2008214>
12. MacDonald NE (2015) Vaccine hesitancy: definition, scope and determinants. *Vaccine 33*: 4161–4164. <https://doi.org/10.1016/j.vaccine.2015.04.036>
13. Buonomo B, Della Marca R, d’Onofrio A, et al. (2022) A behavioural modelling approach to assess the impact of COVID-19 vaccine hesitancy. *J Theor Biol 534*: 110973. <https://doi.org/10.1016/j.jtbi.2021.110973>
14. Imai N, Rawson T, Knock ES, et al. (2023) Quantifying the effect of delaying the second COVID-19 vaccine dose in England: a mathematical modelling study. *Lancet Public Health 8*: e174–e183. [https://doi.org/10.1016/S2468-2667\(22\)00337-1](https://doi.org/10.1016/S2468-2667(22)00337-1)
15. Khan T, Ullah R, Zaman G, et al. (2021) A mathematical model for the dynamics of SARS-CoV-2 virus using the Caputo-Fabrizio operator. *Math Biosci Eng 18*: 6095–6116. <https://doi.org/10.3934/mbe.2021305>
16. Khan T, Qian ZS, Ullah R, et al. (2021) The transmission dynamics of hepatitis B virus via the fractional-order epidemiological model. *Complexity 2021*: 1–18. <https://doi.org/10.1155/2021/8752161>
17. Khan T, Ullah R, Yousef A, et al. (2022) Modeling and dynamics of the fractional order SARS-CoV-2 epidemiological model. *Complexity 2022*. <https://doi.org/10.1155/2022/3846904>
18. Lusekelo E, Helikumi M, Kuznetsov D, et al. (2023) Quantifying the effects of temperature and predation on the growth of Aedes mosquito population. *Model Earth Syst Environ 9*: 3139–3206. <https://doi.org/10.1007/s40808-022-01687-x>
19. Lusekelo E, Helikumi M, Kuznetsov D, et al. (2023) Dynamic modelling and optimal control analysis of a fractional order chikungunya disease model with temperature effects. *Results Control Optim 10*: 100206. <https://doi.org/10.1016/j.rico.2023.100206>
20. Helikumi M, Eustace G, Mushayabasa S (2022) Dynamics of a fractional-order chikungunya model with asymptomatic infectious class. *Comput Math Methods Med 2022*: 5118382. <https://doi.org/10.1155/2022/5118382>
21. Podlubny I (1999) *Fractional Differential Equations: An Introduction to Fractional Derivatives, Fractional Differential Equations, to Methods of their Solution and some of their Applications*, USA: Academic press, 1–340. [https://doi.org/10.1016/s0076-5392\(99\)x8001-5](https://doi.org/10.1016/s0076-5392(99)x8001-5)
22. Dighriri IM, Alhusayni KM, Mobarki AY, et al. (2022) Pfizer-BioNTech COVID-19 vaccine (BNT162b2) side effects: a systematic review. *Cureus 14*: e23526. <https://doi.org/10.7759/cureus.23526>

23. Van den Driessche P, Watmough J (2002) Reproduction number and subthreshold endemic equilibria for compartment models of disease transmission. *Math Biosci* 180: 29–48. [https://doi.org/10.1016/S0025-5564\(02\)00108-6](https://doi.org/10.1016/S0025-5564(02)00108-6)
24. Diekmann O, Heesterbeek JAP, Roberts MG (2010) The construction of next-generation matrices for compartmental epidemic models. *J R Soc Interface* 7: 873–885. <https://doi.org/10.1098/rsif.2009.0386>
25. Ali A, Ullah S, Khan MA (2022) The impact of vaccination on the modeling of COVID-19 dynamics: a fractional order model. *Nonlinear Dyn* 110: 3921–3940. <https://doi.org/10.1007/s11071-022-07798-5>
26. Mumbu ARJ, Hugo AK (2020) Mathematical modelling on COVID-19 transmission impacts with preventive measures: a case study of Tanzania. *J Biol Dyn* 14: 748–766. <https://doi.org/10.1080/17513758.2020.1823494>
27. Marino S, Hogue IB, Ray CJ, et al. (2008) A methodology for performing global uncertainty and sensitivity analysis in systems biology. *J Theor Biol* 254: 178–196. <https://doi.org/10.1016/j.jtbi.2008.04.011>
28. Ahmad S, Ullah A, Partohaghighi M, et al. (2021) Oscillatory and complex behaviour of Caputo-Fabrizio fractional order HIV-1 infection model. *Aims Math* 7: 4778–4792. <https://doi.org/10.3934/math.2022265>
29. Gashirai TB, Hove-Musekwa SD, Mushayabasa S (2021) Dynamical analysis of a fractional-order foot-and-mouth disease model. *Math Sci* 15: 65–82. <https://doi.org/10.1007/s40096-020-00372-3>
30. Nisar KS, Ahmad S, Ullah A, et al. (2021) Mathematical analysis of SIRD model of COVID-19 with Caputo fractional derivative based on real data. *Results Phys* 21: 103772. <https://doi.org/10.1016/j.rinp.2020.103772>
31. Olivera Mesa D, Hogan AB, Watson OJ, et al. (2022) Modelling the impact of vaccine hesitancy in prolonging the need for Non-Pharmaceutical Interventions to control the COVID-19 pandemic. *Commun Med* 2: 14. <https://doi.org/10.1038/s43856-022-00075-x>
32. Yin JDC (2022) Media data and vaccine hesitancy: scoping review. *JMIR Infodemiology* 2: e37300. <https://doi.org/10.2196/37300>
33. Mishra S, Kwong JC, Chan AK, et al. (2020) Understanding heterogeneity to inform the public health response to COVID-19 in Canada. *CMAJ* 192: E684–E685. <https://doi.org/10.1503/cmaj.201112>
34. Li C, Zeng F (2013) The finite difference methods for fractional ordinary differential equations. *Numer Funct Anal Optim* 34: 149–179. <https://doi.org/10.1080/01630563.2012.706673>
35. Odibat ZM, Shawagfeh NT (2007) Generalized Taylor’s formula. *Appl Math Comput* 186: 286–293. <https://doi.org/10.1016/j.amc.2006.07.102>
36. Liang S, Wu R, Chen L (2015) Laplace transform of fractional order differential equations. *Electron J Differ Equ* 139: 2015. <http://ejde.math.txstate.edu>
37. Kexue L, Jigen P (2011) Laplace transform and fractional differential equations. *Appl Math Lett* 24: 2019–2023. <https://doi.org/10.1016/j.aml.2011.05.035>

-
38. LaSalle JP (1976) *The Stability of Dynamical Systems*, Philadelphia: SIAM. <https://doi.org/10.1137/1.9781611970432>.
39. Vargas-De-León C (2015) Volterra-type Lyapunov functions for fractional-order epidemic systems. *Commun Nonlinear Sci* 24: 75–85. <https://doi.org/10.1016/j.cnsns.2014.12.013>



AIMS Press

© 2023 the Author(s), licensee AIMS Press. This is an open access article distributed under the terms of the Creative Commons Attribution License (<http://creativecommons.org/licenses/by/4.0>)